

This is a repository copy of *First observation of the decay of the $13/2^+$ isomer in 183Hg and $B(M2)$ systematics of neutron transitions across the nuclear chart.*

White Rose Research Online URL for this paper:

<https://eprints.whiterose.ac.uk/189681/>

Version: Published Version

Article:

Huang, H., Zhang, W.Q., Andreyev, A.N. orcid.org/0000-0003-2828-0262 et al. (40 more authors) (2022) First observation of the decay of the $13/2^+$ isomer in 183Hg and $B(M2)$ systematics of neutron transitions across the nuclear chart. *Physics Letters B.* 137345. ISSN 0370-2693

<https://doi.org/10.1016/j.physletb.2022.137345>

Reuse

This article is distributed under the terms of the Creative Commons Attribution (CC BY) licence. This licence allows you to distribute, remix, tweak, and build upon the work, even commercially, as long as you credit the authors for the original work. More information and the full terms of the licence here:

<https://creativecommons.org/licenses/>

Takedown

If you consider content in White Rose Research Online to be in breach of UK law, please notify us by emailing eprints@whiterose.ac.uk including the URL of the record and the reason for the withdrawal request.



First observation of the decay of the $13/2^+$ isomer in ^{183}Hg and $B(M2)$ systematics of neutron transitions across the nuclear chart

H. Huang^{a,b}, W.Q. Zhang^{a,b}, A.N. Andreyev^{c,d,*}, Z. Liu^{a,b,**}, D. Seweryniak^e, Z.H. Li^f, C.Y. Guo^f, A.E. Barzakh^h, P. Van Duppenⁱ, B. Andel^j, S. Antalic^j, M. Block^{k,l,m}, A. Bronis^j, M.P. Carpenter^e, P. Copp^e, J.G. Cubiss^c, B. Ding^{a,b}, D.T. Doherty^g, Z. Favierⁿ, F. Giacoppo^{k,l}, T.H. Huang^{a,b,e}, B. Kindler^l, F.G. Kondev^e, T. Lauritsen^e, J.G. Li^{a,b}, G.S. Li^{a,b}, B. Lommel^l, H.Y. Lu^{a,b}, M. Al Monthery^c, P. Mořatř^j, Y.F. Niu^o, C. Raison^c, W. Reviol^e, G. Savard^e, S. Stolze^e, G.L. Wilson^p, H.Y. Wu^f, Z.H. Wang^o, F.R. Xu^f, Q.B. Zeng^{a,b}, X.H. Yu^{a,b}, F.F. Zeng^{a,b}, X.H. Zhou^{a,b}

^a Institute of Modern Physics, Chinese Academy of Sciences, Lanzhou 730000, China

^b University of Chinese Academy of Sciences, Beijing 100049, China

^c Department of Physics, University of York, York, YO10 5DD, United Kingdom

^d Advanced Science Research Center (ASRC), Japan Atomic Energy Agency, Tokai-mura, Japan

^e Physics Division, Argonne National Laboratory, Argonne, IL 60439, USA

^f State Key Laboratory of Nuclear Physics and Technology, School of Physics, Peking University, Beijing 100871, China

^g Department of Physics, University of Surrey, Guildford, GU2 7XH, United Kingdom

^h Petersburg Nuclear Physics Institute, NRC Kurchatov Institute, 188300 Gatchina, Russia

ⁱ KU Leuven, Instituut voor Kern- en Stralingsfysica, 3001 Leuven, Belgium

^j Department of Nuclear Physics and Biophysics, Comenius University in Bratislava, 84248 Bratislava, Slovakia

^k Helmholtz-Institut Mainz, Mainz, 55128, Germany

^l GSI Helmholtzzentrum für Schwerionenforschung Darmstadt, Darmstadt, 64291, Germany

^m Johannes-Gutenberg Universität, Mainz, 55099, Germany

ⁿ Physics Department, CERN, 1211 Geneva 23, Switzerland

^o Lanzhou University, Lanzhou 730000, China

^p Department of Physics and Astronomy, Louisiana State University, Baton Rouge, LA 70803, USA

ARTICLE INFO

Article history:

Received 21 March 2022

Received in revised form 18 July 2022

Accepted 20 July 2022

Available online 25 July 2022

Editor: B. Blank

Keywords:

Isomeric decay

Shape isomer

$B(M2)$

ABSTRACT

The decay of the $13/2^+$ isomeric state in ^{183}Hg was observed for the first time following the α decay of the $13/2^+$ isomer in ^{187}Pb produced in the $^{142}\text{Nd}(^{50}\text{Cr}, 2p3n)$ reaction. Using $\alpha - \gamma$ delayed coincidence measurements, the half-life of this isomer was measured to be $290(30) \mu\text{s}$. This isomer is proposed to deexcite by an unobserved low-energy $M2$ transition to the known $9/2^-$ member of a strongly prolate-deformed $7/2^- [514]$ band, followed by a 105-keV $M1$ transition to the bandhead. A lower limit of $B(M2) \geq 0.018$ W.u. was deduced for the unobserved transition. The presumed retardation is proposed to be due to the notable shape change between the initial, nearly spherical, and the final, strongly deformed, states. A similar scenario is also considered for the $13/2^+$ isomer in ^{181}Hg , suggesting both are cases of shape isomers. The $B(M2)$ systematics of neutron transitions across the nuclear chart is discussed.

© 2022 The Author(s). Published by Elsevier B.V. This is an open access article under the CC BY license (<http://creativecommons.org/licenses/by/4.0/>). Funded by SCOAP³.

* Corresponding author at: Department of Physics, University of York, York, YO10 5DD, United Kingdom.

** Corresponding author at: Institute of Modern Physics, Chinese Academy of Sciences, Lanzhou 730000, China.

E-mail addresses: andrei.andreyev@york.ac.uk (A.N. Andreyev), liuzhong@impcas.ac.cn (Z. Liu).

<https://doi.org/10.1016/j.physletb.2022.137345>

0370-2693/© 2022 The Author(s). Published by Elsevier B.V. This is an open access article under the CC BY license (<http://creativecommons.org/licenses/by/4.0/>). Funded by SCOAP³.

1. Introduction

Isomeric states, first observed about 100 years ago [1,2], play an important role in nuclear physics [3–5]. Some of them also provide opportunities in applications, e.g., for medical imaging and energy storage [3–6]. As valuable probes of nuclear structure, such metastable states can be classified into shape isomers, spin isomers, K isomers and seniority isomers based on the inhibition

mechanism [2,3,7–10]. For shape isomers, the hindrance mainly results from the distinct shape change between initial and final states [3–5]. A global study based on the macroscopic-microscopic model predicted that an island of shape-isomers may exist around the proton shell closure at $Z = 82$ near the neutron $N = 104$ mid-shell, see Fig. 5 in Ref. [11].

The $13/2^+$ isomers originating from the $\nu i_{13/2}$ orbit are widespread in the $N = 82$ –126 region [12], where they have been observed in many even- Z , odd- A Er-Th isotopes. Decay paths of such isomers have been also reported in a chain of odd- A 175 – 199 Hg isotopes, except for ^{183}Hg [13–23]. In 185 – 199 Hg, the half-lives of these isomers are sufficiently long (seconds or longer) to allow for determinations of the changes in their mean-squared charge radii via isotope shift experiments. These isomers were deduced to be nearly spherical ($(\beta_2^2)^{1/2} \sim 0.1$) [24–26], albeit in the literature they are often also claimed to be “weakly oblate”, with a $13/2^+[606]$ configuration. Such isomers become short-lived in the lighter odd- A isotopes 175 – 181 Hg, with typical half-lives in the μs - and sub- μs range [13–15,27], which prevents measurements of mean-squared charge radii. Based on their decay pattern and potential energy surface (PES) calculations, they were also interpreted as nearly spherical (or weakly-oblate) as in the heavier isotopes [13,14,16–18]. The main decay modes of these isomers change from charged-particle decay in 187 – 193 Hg to internal transition (IT) in 175 – 181 . ^{185}Hg .

In ^{183}Hg , a long-lived $1/2^-$ [521] ground state (g.s.) with prolate deformation is known [25,28], together with a $13/2^+$ isomeric state [27,29], denoted as ^{183m}Hg in this work. However, the decay path of this isomer was not known prior to the present study. Its existence was proposed based on the presumably unhindered 6077(7)-keV α decay¹ of the $13/2^+$ isomer in ^{187}Pb in a study [30], which stated “It is more likely that it represents a favored transition to a $13/2^+$ level in ^{183}Hg , which then has a lifetime which is appreciably longer than the coincidence time of 8 μs applied in our studies.” The unhindered nature of the 6077-keV decay was directly confirmed in the α -decay investigation of $^{191}\text{Po} \rightarrow ^{187}\text{Pb} \rightarrow ^{183}\text{Hg}$ (see Fig. 2 of Ref. [31]), whereby ^{183m}Hg was proposed to have a $\nu i_{13/2}$ configuration that is weakly coupled to the nearly spherical $\pi(0p-2h)$ ^{182}Hg core. Combining the α -decay data [30] with mass-measurements [32] for the $13/2^+$ isomer and $1/2^-$ g.s. in ^{187}Pb , an excitation energy of $E^*(13/2^+, ^{183m}\text{Hg}) = 204(14)$ keV was evaluated in Ref. [29].

In the present work, the first observation of the decay from ^{183m}Hg is presented via identification of its IT decay, following the α decay of the $13/2^+$ isomer in ^{187}Pb . The present result comes from the same experiment, in which prompt and delayed γ spectroscopy of ^{187}Pb was performed [33].

2. Experiment

The parent nuclei ^{187}Pb were produced via the $^{50}\text{Cr} + ^{142}\text{Nd} \rightarrow ^{192}\text{Po}^* \rightarrow ^{187}\text{Pb} + 2p3n$ fusion-evaporation reaction. The ^{50}Cr ions were accelerated to 255 MeV, with a typical intensity of 7 particle nA by the superconducting linear accelerator, ATLAS, at Argonne National Laboratory (ANL). Targets with a thickness of $\sim 700 \mu\text{g}/\text{cm}^2$ (including fluorine) were prepared from $^{142}\text{NdF}_3$ material with an isotopic enrichment of $\sim 99.8\%$. To reduce possible degradation of the target due to beam heating, four target sectors were mounted on a rotating wheel, and a magnetic steerer was used to wobble the beam ± 2.5 mm horizontally across the target [15].

¹ Evaluated value from [27], the original data from Ref. [30] was 6073(10) keV, $T_{1/2} = 18.3(3)$ s, no α -branching was deduced.

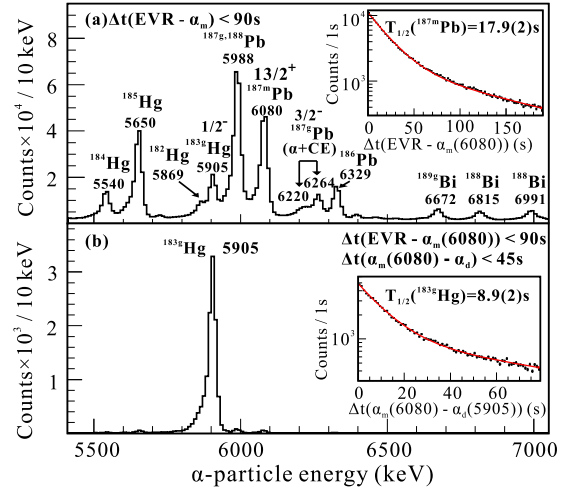


Fig. 1. (a) A part of the energy spectrum for the α particles recorded within 90 s after EVR implantation. (b) Daughter α -decay spectrum from the $\text{EVR} - \alpha_m(6080) - \alpha_d$ correlations. The α -decay peaks are labeled with their energy in keV and the isotopes they belong to. The $\text{EVR} - \alpha_m(6080)$ time distribution of the ^{187m}Pb decay and the $\alpha_m(6080) - \alpha_d$ time distribution from the $\text{EVR} - \alpha_m(6080) - \alpha_d$ correlations are shown in the insets of (a) and (b), respectively. Since the random contribution is non-negligible, the time distributions are fitted using two exponential functions, and shown by red solid lines.

The recoiling fusion evaporation residues (EVRs) were separated from unwanted particles (projectiles, scattered target nuclei, transfer reaction products) by the Argonne Gas-Filled Analyzer (AGFA), filled with ~ 0.65 mbar helium gas [34]. After separation, EVRs were implanted into a 160×160 (64×64 mm², $\sim 300 \mu\text{m}$ thick) double-sided silicon strip detector (DSSD). The energy calibration of the DSSD was performed by using α -decay peaks of known, strongly produced activities from this reaction, see Fig. 1(a). The α decays of ^{183}Hg (5904(5) keV), ^{184}Hg (5539(5) keV), ^{185}Hg (5653(5) keV), ^{186}Pb (6331(6) keV), ^{187m}Pb (6077(7) keV), ^{188}Bi (6992(5) keV and 6813(5) keV) and ^{189}Bi (6670.9(22) keV), evaluated in Ref. [27], were used. With this calibration, we reproduce the energies of all peaks, shown in Fig. 1, within 1–3 keV, and the measured energies will be used in the text. The typical energy resolution for the strips of the DSSD was ~ 30 keV (FWHM) for 5000–7000 keV α particles. The energy, position and time of the implantation of EVRs and their subsequent α decays were registered. A position-sensitive parallel grid avalanche counter (PGAC) was installed upstream of the DSSD. The coincidence between signals from the PGAC and the DSSD enabled implantation of ions to be distinguished from decays. Gamma rays emitted from the EVRs and their daughters were detected by four HPGe clover detectors (X-array) surrounding the DSSD [35]. The absolute detection efficiencies of the X-array were deduced as $\varepsilon_\gamma(70 \text{ keV}) \sim 8\%$, $\varepsilon_\gamma(100 \text{ keV}) \sim 19\%$ and $\varepsilon_\gamma(300 \text{ keV}) \sim 14\%$. The ‘software’ threshold of X-array was ~ 20 keV, and its resolution was ~ 2.8 keV (FWHM) at 100 keV. The data were recorded by using the digital data acquisition system, consisting of 100-MHz 14-bit sampling ADCs, and analyzed using the CERN ROOT framework [36].

3. Results

3.1. α -decay analysis

A part of the α -decay spectrum registered in the DSSD, for the events following the implantation of EVRs within 90 s in the same pixel, is shown in Fig. 1(a). The 6080(4) keV peak labeled as ^{187m}Pb in Fig. 1(a), with $\sim 1.3 \times 10^5$ counts, was associated with the known α decay of the $13/2^+$ isomer in ^{187}Pb to ^{183m}Hg .

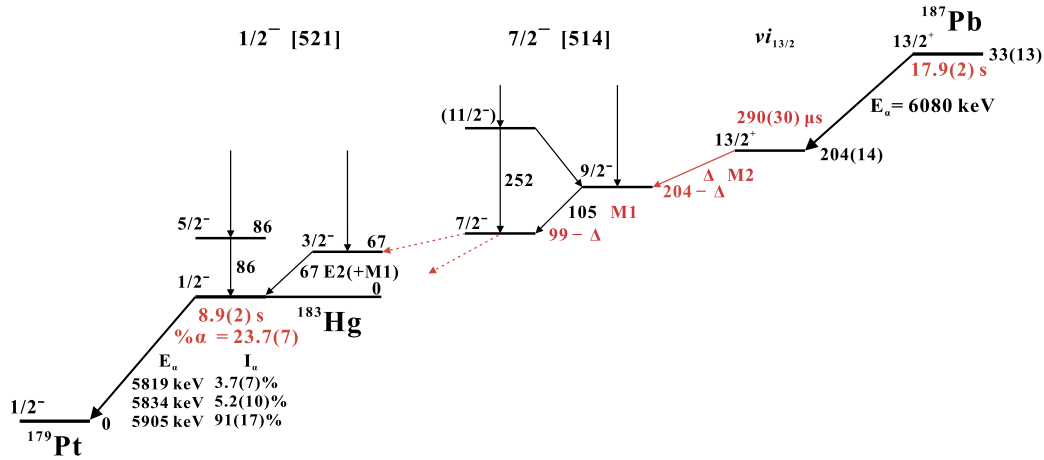


Fig. 2. Partial α -decay schemes of ^{187m}Pb and ^{183g}Hg , and of γ decays of low-lying states in ^{183g}Hg . The known data are shown in black and taken from Refs. [19–21,27]. The positions of $3/2^-$ and $5/2^-$ are given as proposed in Ref. [19], which is slightly different from Ref. [20] (see the evaluation of Ref. [27]). The new data from this study are shown in red. The evaluated excitation energy of $E^* = 204(14)$ keV is from Ref. [29]. The Δ transition, albeit yet unobserved, must exist, it is shown by red solid line. The possible decay paths of the $7/2^-$ level are shown by the red dashed lines, for the cases of $\Delta < 32(14)$ keV see Sec. 4.2 for details.

The main α -decay peak of the $1/2^-$ g.s. in ^{183}Hg is also seen at 5905(4) keV.² The time distribution between the recoil implantation and subsequent 6080-keV decay is shown in the inset of Fig. 1(a). A half-life of $T_{1/2}(^{187m}\text{Pb}) = 17.9(2)$ s was deduced, in good agreement with the literature value of 18.3(3) s [30].

The α decay of the daughter isotope ^{183}Hg , following the 6080-keV decay of ^{187}Pb was investigated through the EVR – $\alpha_m(6080) - \alpha_d$ correlations. The obtained α_d energy spectrum is shown in Fig. 1(b), where the 5905(4)-keV decay from the $1/2^-$ g.s. of ^{183}Hg is clearly observed. This proves that the decay of the $13/2^+$ isomer in ^{183}Hg proceeds, at least partially, via an IT cascade to the $1/2^-$ g.s. of ^{183}Hg (see the decay scheme in Fig. 2). This decay must involve several transitions in a cascade, as a single $13/2^+ \rightarrow 1/2^-$ transition would require an $M6$ and/or $E7$ multipolarity, which would have a very long half-life ($> 10^{12}$ years) for a realistic energy range limited by the 204(14)-keV excitation energy of the $13/2^+$ isomer in ^{183}Hg . We also point out that the study of Misaelidis et al. [30] suggested that the lifetime of this state should be longer than 8 μs .

By comparing the number of 6080-keV decays in Fig. 1(a) with those of the 5905-keV peak (also including the two fine-structure decays) from Fig. 1(b), an α -decay branching ratio of $b_\alpha(^{183g}\text{Hg}) = 23.7(7)\%$ was deduced, which is in agreement with 25.5(15)% from Refs. [27,37], but is discrepant with the evaluated value of 11.7(20)% [27]. The time distribution of the 5905-keV decay is presented in the inset of Fig. 1(b). The extracted value of $T_{1/2}(^{183g}\text{Hg}) = 8.9(2)$ s is in agreement with the evaluated value of 9.4(7) s [27], but more precise.

We performed simulations of the time distribution for the 5905-keV decay deduced from the experimental $\alpha - \alpha$ correlation method, by assuming the presence of possible intermediate isomeric state within the IT cascade and by varying its half-life. This could be either the $13/2^+$ state in ^{183}Hg itself, or any other isomeric states in its IT decay. Based on the comparison between the simulated and experimental decay distributions for the 5905-keV line, an upper limit of ~ 0.1 s was deduced for such an intermediate state. For longer half-lives, the two distributions become incompatible, due to the presence of the growing component in the simulated time distribution, which is absent in the experimental plot in the inset of Fig. 1(b). These suggest that the half-lives of the $13/2^+$ isomer itself and/or other additional states within its

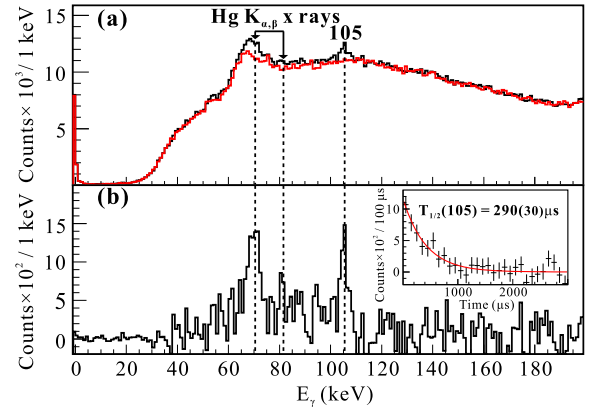


Fig. 3. (a) Black histogram: the γ -ray energy spectrum collected within $0.6 \mu\text{s} < \Delta t(\alpha_m(6080)-\gamma) < 1200 \mu\text{s}$. Red histogram: the time-random spectrum for the interval $-1200 \mu\text{s} < \Delta t(\alpha_m(6080)-\gamma) < -0.6 \mu\text{s}$. (b) The background subtracted γ -ray energy spectrum [difference of the two spectra in panel (a)]. The inset of panel (b) shows the background subtracted time distribution for the 105-keV delayed γ -ray transition in ^{183g}Hg within $\Delta t[\alpha_m(6080)-\gamma(105)] = 0-3000 \mu\text{s}$. A least-squares fit was performed for the exponential decay, and shown by the red line.

decay path should be less than 0.1 s, which will be important for the discussion of the decay scheme in Sec. 4.

3.2. IT decay of ^{183m}Hg

Next, an $\alpha_m(6080) - \gamma$ correlation analysis was performed to investigate the IT decay from the $13/2^+$ isomer to the $1/2^-$ g.s. in ^{183}Hg . A time window of $0.6 < \Delta t(\alpha_m(6080)-\gamma) < 1200 \mu\text{s}$ was used to avoid contamination from prompt $\alpha_m - \gamma$ coincidences following the α decay of ^{187g}Pb to excited states in its daughter. The corresponding spectrum is shown in black in Fig. 3(a). The time-random background spectrum, shown in red in Fig. 3(a), was obtained by applying a reverse time gate of $-1200 < \Delta t(\alpha_m(6080)-\gamma) < -0.6 \mu\text{s}$. The difference between these two spectra is presented in Fig. 3(b), where the Hg $K_{\alpha,\beta}$ X rays and a γ -ray peak at 105.2(2) keV are clearly seen. The inset of Fig. 3(b) is a time distribution $\Delta t[\alpha(6080)-\gamma(105)]$, after subtracting the reverse counterpart. Based on a least-squares fit of this time distribution with an exponential function, a half-life of $T_{1/2}(105 \text{ keV}) = 290(30) \mu\text{s}$ was extracted. This long value explains the non-observation of the IT cascade in the experiment of Misaelidis et al. [30]. The 105-keV transition is a γ decay observed for the first

² There are also weak fine-structure α -decays of ^{183g}Hg , shown in the decay scheme in Fig. 2, with the energies of 5819(10) keV and 5834(10) keV.

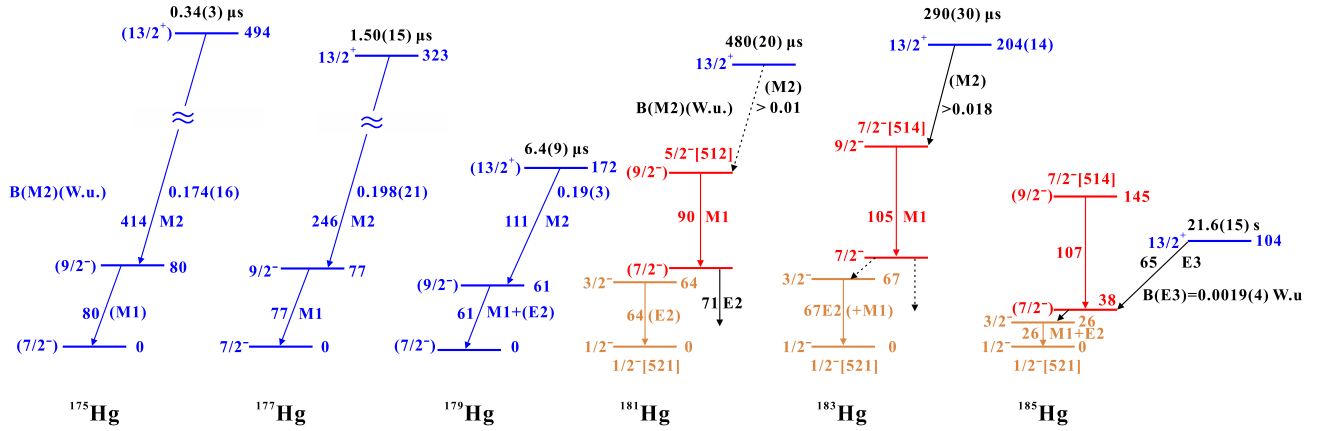


Fig. 4. The decay paths of the $13/2^+$ isomers in odd- A $^{175-185}\text{Hg}$ [13–15,19,22,27], the levels energies in ^{185}Hg are from Ref. [23]. The decay path of the $7/2^-$ level in ^{183}Hg is shown as in Fig. 2. Different structures/bands are shown in different colors, all near-spherical states are drawn in blue. In $^{175,177,179}\text{Hg}$, the g.s. and the first excited states are proposed to be near-spherical and likely have the $f_{7/2}$ and $h_{9/2}$ single-particle configurations, respectively [13,14,16]. In $^{181,183,185}\text{Hg}$, the prolate $1/2^- [521]$ g.s. bands are shown in orange, while the $5/2^- [512]$ and $7/2^- [514]$ prolate bands are plotted in red. The Weisskopf single-particle transition probabilities of the decays deexciting the $13/2^+$ isomers are shown.

time in the expected IT cascade from ^{183m}Hg , its placement as shown in Fig. 2 will be discussed in Sec. 4.

No γ or Hg $K_{\alpha,\beta}$ X ray was found in coincidence with the 105-keV transition in a $\gamma - \gamma$ coincidence analysis, indicating that all other transitions in the expected $13/2^+ \rightarrow 1/2^-$ g.s. decay path are either very low in energy (below the registration threshold) and/or very strongly converted. Based on the known excitation energy of $E^*(13/2^+) = 204(14)$ keV, the missing γ -ray transitions in the IT cascade should have a sum energy of $204(14) - 105.2(2) = 99(14)$ keV. As will be discussed in Sec. 4, at least two extra transitions, one depopulating the $13/2^+$ isomer (shown by a solid red arrow and denoted as Δ in Fig. 2) and another depopulating the $7/2^-$ level (shown by the dashed lines in Fig. 2) should be present, thus it is highly likely that their energies are below the Hg K -shell electron binding energy (83 keV [38]). Therefore, we assume that all Hg $K_{\alpha,\beta}$ X rays in Fig. 3(b) originate from the internal conversion of the 105-keV transition. Under this assumption, a K -shell internal conversion coefficient (ICC) $\alpha_{K,exp}(105 \text{ keV}) = 5.7(3)$ was deduced, by comparing the numbers of the Hg $K_{\alpha,\beta}$ X rays and the 105-keV γ rays in Fig. 3(b), both normalized by the respective γ -ray detection efficiencies. This value establishes an $M1$ multipolarity for the 105-keV transition, as the experimental value matches well to the theoretical $M1$ value of $\alpha_{K,th}(M1) = 5.6$ ($\alpha_{K,th}(E1) = 0.3$, $\alpha_{K,th}(E2) = 0.6$ and $\alpha_{K,th}(M2) = 37$) [39]. Such inference is also supported by the value of the total ICC, $\alpha_{tot,exp}(105 \text{ keV}) = 6.3(6)$, derived from comparing the numbers of 6080-keV α decays in Fig. 1(a) and the $\alpha(6080) - \gamma(105)$ correlations in Fig. 3(b), after accounting for the detection efficiency for this γ ray. The theoretical total ICCs are $\alpha_{tot,th} = 0.37$ ($E1$), 6.8 ($M1$), 4.5 ($E2$), 55.8 ($M2$) [39]. Considering the experimental uncertainties of both $\alpha_{K,exp}$ and $\alpha_{tot,exp}$, we conclude that the 105-keV transition has an $M1$ character.

4. Discussion

4.1. The decay path of the $13/2^+$ isomer

In ^{183}Hg , several prolate-deformed rotational bands have been established experimentally [19–21], e.g., the $1/2^- [521]$ g.s. band and a “floating” $7/2^- [514]$ band, which are also known in the neighboring deformed nuclides, e.g., $^{181,185}\text{Hg}$ and $^{181,183}\text{Pt}$ [27]. Selected low-lying levels from these bands, of possible relevance to the decay of the $13/2^+$ isomer, are shown in Fig. 2. In previous studies, a prompt 104.9(2)-keV γ ray was assigned as the $9/2^- \rightarrow 7/2^-$ $M1/E2$ member of the $7/2^- [514]$ band [19,20]. Having

similar energy and multipolarity with the 105.2(2)-keV transition observed in the present work, we assume that they are the same transition. Therefore, the most likely scenario is that the prompt 105-keV $9/2^- \rightarrow 7/2^- [514]$ decay is preceded by an unobserved $13/2^+ \rightarrow 9/2^-$ transition from the 290- μs isomer, denoted as Δ in Fig. 2.

Given the proposed placement, the multipolarity of the Δ decay should be $M2$, possibly, mixed with $E3$. Furthermore, an upper energy limit of $\Delta \leq 83$ keV can be established, as a higher value would allow a K -shell conversion for this transition (Hg K -shell electron binding energy is 83 keV [38]), with a high K -conversion coefficient, e.g. $\alpha_k(85 \text{ keV}, M2) = 77$ [39]. However, this is ruled out by the amount of Hg K X rays in Fig. 3. Based on the Weisskopf single particle half-life estimates [38], the lower half-life limit of ~ 56 ms for a pure unhindered 83-keV $E3$ transition should be four orders of magnitude longer than ~ 5 μs for a pure unhindered $M2$ 83-keV decay, which limits an $E3$ admixture for the Δ transition. As a relevant example, we refer to the pure $E3$ $13/2^+ \rightarrow 7/2^-$ transition with a comparable energy of 65 keV in ^{185}Hg (see Fig. 4), which has a half-life of 21.6(15) s and is strongly hindered ($B(E3) = 0.0019(4)$ W.u.).

Based on the same reasoning, a direct $E3$ $\Delta + 105$ keV, $13/2^+ \rightarrow 7/2^- [514]$ transition, with an energy range of 105–188 keV, can also be ruled out.

4.2. Possible decay paths of the $7/2^-$ state at 99 – Δ keV

The decay of the $7/2^- [514]$ state at 99(14) – Δ keV (see Fig. 2) is an opened question. None of the previous prompt γ -decay studies [19–21] were able to establish its decay path and excitation energy. Furthermore, slightly different placements of the $3/2^-$ and $5/2^-$ excited states in the $1/2^- [521]$ band were proposed in Refs. [19,20], (see the discussion in the evaluation [27]). In Fig. 2, they are shown as proposed in the adopted level scheme in Ref. [27].

If $\Delta \geq 32(14)$ keV, the $7/2^-$ will be below the known $3/2^-$ state at 67 keV, thus a direct $M3$ $7/2^- \rightarrow 1/2^-$ transition with an energy of less than 67 keV is possible. This scenario occurs in ^{181}Os and ^{183}Pt (see supplementary material [40]), where $M3$ decays with comparable energies of 49 and 35 keV become isomeric, with half-lives of 2.7(1) min and 43(5) s, respectively. Such a scenario for ^{183}Hg should be ruled out based on our estimate of the upper half-life limit of 0.1 s, derived from $\alpha - \alpha$ correlations. However, if some additional low-lying state(s) exist(s) below the $7/2^-$ state, as e.g. the $3/2^-$ level at 26 keV in ^{185}Hg (Fig. 4), then

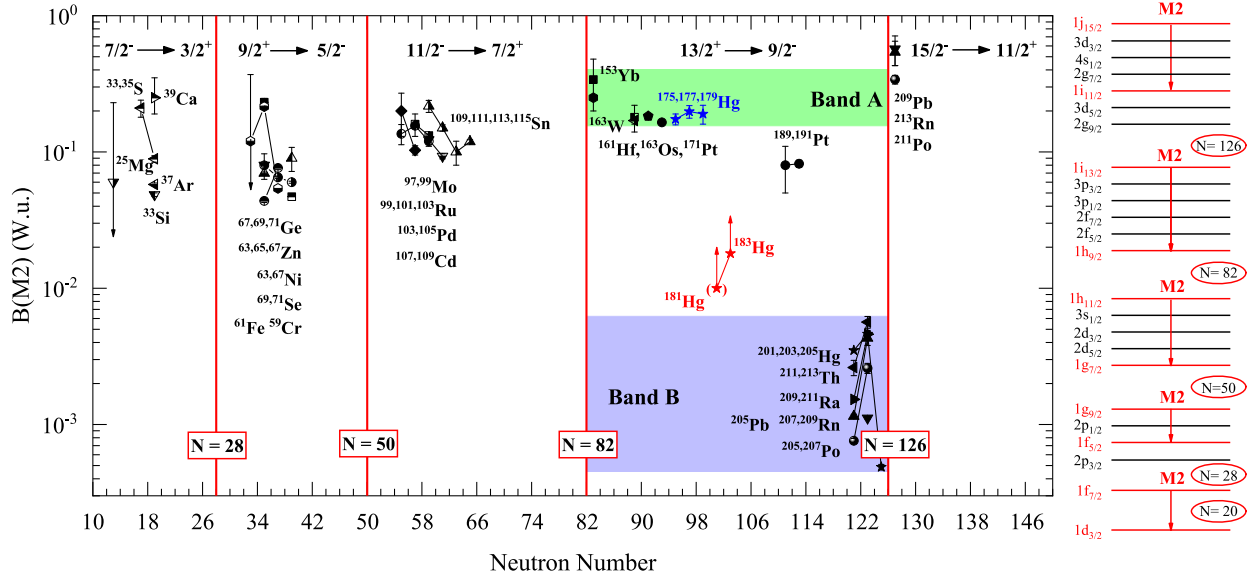


Fig. 5. Right panel: The schematic representation of the spherical single-particle neutron orbitals for a modified harmonic oscillator [38]. The orbitals involved in the $M2$ -decays in different shells are shown in red. Left panel: The $M2$ transition probabilities in Weisskopf units for the $7/2^-$, $9/2^+$, $11/2^-$ and $13/2^+$ isomers in the even- Z , odd- N isotopes [27,29]. The lower limits for $B(M2)$ in $^{181,183}\text{Hg}$ from this work are shown with red stars. In the $N = 82$ -126 valence space, they are divided into band A and band B (see Sec. 4.4 for details).

the $7/2^-$ state can decay by a prompt, strongly converted path to the $1/2^-$ ground state. Such a decay would be unobservable in the present experiment, due to strong internal conversion and low γ -ray detection efficiency at such energies.

If $\Delta \leq 32(14)$ keV, the $7/2^-$ state will be above the $3/2^-$ state at 67 keV or even above the $5/2^-$ state at 86 keV. In this case, the respective $E2$ $7/2^- \rightarrow 3/2^-$ and $M1$ $7/2^- \rightarrow 5/2^-$ decays will be K -hindered, due to their $\nu = \Delta K(3) - \lambda(2) = 1$ and $\nu = \Delta K(3) - \lambda(1) = 2$ characters, respectively, where ΔK is the K -value difference between the two bandhead states, and λ is the transition angular momentum [10]. Using the expressions given in Sec. 6 of Ref. [10], a typical hindrance factors of ~ 400 and 8×10^5 can be deduced for these transitions. Therefore, the half-lives will be ~ 80 μs and ~ 2 μs for the representative energy range of 20-30 keV. Indeed, such $M1$ transitions in ^{179}Os and ^{181}Pt are strongly hindered ($B(M1) \sim (4-7) \times 10^{-5}$ W.u.) (see supplementary material [40]). Such long values, along with low γ -ray energies and high internal conversion could explain non-observations of these transitions in ^{183}Hg .

Despite the usage of the digital data acquisition system in the present experiment, which allowed a search for delayed γ - γ coincidences, no evidence for such decays, or for possible follow-up 67- and 86-keV decays was found. This could be explained by the amount of statistics in our study, as e.g. only ~ 10 $\gamma(105)$ - $\gamma(67)$ coincidences would be expected in the present study after accounting for the internal conversion and γ -ray registration efficiency.

Future experiments with dedicated low-energy γ -ray and internal conversion electron detection, similar as applied for the study of ^{189}Pb and ^{185}Hg in Ref. [23] can help to resolve this issue.

4.3. Systematics of $13/2^+ \rightarrow 9/2^-$ isomeric $M2$ transitions in odd A $^{175-183}\text{Hg}$ isotopes

Based on the upper limit of 83 keV for the Δ transition and its measured half-life of 290(30) μs , a lower limit for the Weisskopf single-particle transition probability, $B(M2, 83 \text{ keV}) = 0.018$ W.u., was deduced. For comparison and to show the sensitivity to Δ , a value of $B(M2, 20 \text{ keV}) = 0.031(3)$ W.u. can be deduced if $\Delta = 20$ keV. The two values suggest a possible hindrance of

$\frac{B(M2, ^{175,177,179}\text{Hg})}{B(M2, ^{183}\text{Hg})} \leq 6-12$ for the Δ transition relative to the typical values of $B(M2) \sim 0.174-0.198$ W.u. in $^{175,177,179}\text{Hg}$, shown in Fig. 4.

We remind that previous studies at the RITU gas-filled separator [13,14,16] considered the $13/2^+ \rightarrow 9/2^-$ transitions in $^{175,177,179}\text{Hg}$ as proceeding between the nearly spherical (or, weakly-oblate) initial isomeric states originating from the $\nu i_{13/2}$ orbital and $\nu h_{9/2}$ spherical final states. According to the authors, small shape change could be responsible for their moderate hindrance with typical values of $B(M2)$ as given in Fig. 4. However, as will be shown in Sec. 4.4, we will argue that such weakly-hindered $B(M2)$ values should be considered as a norm of the neutron single-particle $M2$ transitions between near-spherical states in the $N = 82$ -126 major shell.

In contrast to $^{175,177,179}\text{Hg}$, in ^{183}Hg , the $9/2^-$ final state is a member of a strongly deformed rotational $7/2^-$ [514] band (shown in red in Fig. 4), with $\beta_2 \sim 0.25$ [21]. This strong shape change between the presumably spherical $13/2^+$ state and the strongly deformed $9/2^-$ state is most likely the reason for the possible stronger hindrance, deduced in the present study. This suggests that the $13/2^+$ state in ^{183}Hg is most probably a shape isomer.

As a relevant example, we quote the case of ^{185}Hg , where the decay from the nearly spherical $13/2^+$ state to the prolate $7/2^-$ [514] bandhead (shown in red in Fig. 4) is also strongly hindered, with $B(E3) = 0.0019(4)$ W.u. [22,23,27].

In the neighboring ^{181}Hg isotope, a 0.48(2)-ms $13/2^+$ isomer was identified in the study at the SHIP separator [18]. Two possible scenarios for the decay from this isomer, via a cascade of three $\Delta - 90.3$ -keV ($M1$) - 71.4-keV ($E2$) transitions (see Fig. 3 of Ref. [18]), were considered, with an upper energy limit of $\Delta \leq 83$ keV, similar to the case of ^{183}Hg . The possibilities of either an $E3$ or $M2$ multipolarity for the delayed Δ transition were discussed, any of which would explain the isomeric nature of this $13/2^+$ state; the authors opted for the $E3$ multipolarity as the most likely [18]. However, we now propose that, by a strong analogy with our new results for ^{183}Hg , the $M2$ multipolarity should

³ The near-sphericity of the $13/2^+$ state is confirmed both by its charge radii and magnetic moment measurements, see Refs. [24-26].

be considered for the Δ decay in ^{181}Hg . In this scenario (earlier discarded in Ref. [18]), the 90.3-keV decay should represent the previously unobserved 91-keV $9/2^- \rightarrow 7/2^-$ transitions within the $5/2^-$ [512] band [17]. The 71.4-keV decay should then proceed to some new low-lying state in ^{181}Hg , but no solid conclusions can be made based on currently available data. A lower limit of $B(M2, 83 \text{ keV}, ^{181}\text{Hg}) \geq 0.01 \text{ W.u.}$ was now deduced and is shown in a bracket as tentative in Fig. 5 due to the indirect nature of the $M2$ multipolarity deduction. The possible hindrance can also be explained by the shape change between initial and final states, as the $5/2^-$ [512] band was also proposed to be strongly prolate [17]. Future γ -ray and internal conversion electron spectroscopy experiments as mentioned for ^{183}Hg in Sec. 4.2 can also help to clarify the decay path.

4.4. The systematics of $B(M2)$ for neutron transitions across the nuclear chart

The right panel of Fig. 5 shows schematically the shell-model orbitals for a modified harmonic oscillator potential, taken from Appendix H of Ref. [38]. The orbitals which might be responsible for single-particle $M2$ isomeric transitions are shown in red. The $B(M2)$ values of all known (to the best of our knowledge) isomers, involving these transitions, are shown in the left panel.

In the $N = 82$ -126 major shell, which is of our main interest, 23 $13/2^+$ isomers deexciting to the $9/2^-$ states by $M2$ transitions are known. The $B(M2)$ of these decays are shown by black (blue for $^{175,177,179}\text{Hg}$ isotopes and red for $^{181,183}\text{Hg}$) symbols in the left panel of Fig. 5. They can be divided into bands A and B with distinctly different $B(M2)$ values. The $B(M2)$ values are $\sim 0.2(1) \text{ W.u.}$ in Band A, while nearly two orders of magnitude smaller in Band B. In Band A, the $13/2^+$ initial and $9/2^-$ final states are of predominantly spherical or nearly spherical single particle character, as e.g. in $^{175,177,179}\text{Hg}$, with no or only a small shape change. So the $M2$ transitions in Band A are actually normal. In contrast, in Band B these isomers are assigned as predominant neutron-hole states ($\nu i_{13/2}^-$), while the configurations of the $9/2^-$ final states are dominated by $|\nu f_{5/2} \otimes 2^+\rangle$ weakly mixed with $|\nu h_{9/2}^- \otimes 0^+\rangle$, as e.g. in ^{201}Hg [41]. The $M2$ transition is only allowed in the latter component, resulting in extremely strong hindrances for such decays [41–43].

The $13/2^+ \rightarrow 9/2^-$ $M2$ transitions in $^{181,183}\text{Hg}$ are situated in between Bands A and B in Fig. 5, their possible hindrance could be caused by shape changes. The decays in $^{189,191}\text{Pt}$ are weakly hindered relative to Band A, which could be explained by the shape change between triaxial initial and prolate final states [44–47].

In other major shells shown in Fig. 5, the $M2$ transitions deexciting the $7/2^-$, $9/2^+$, $11/2^-$ and $15/2^-$ isomers in even- Z , odd- N isotopes have $B(M2)$ values similar to those in Band A for the normal $13/2^+ \rightarrow 9/2^-$ decays, with the bulk of data around 0.1–0.2 W.u. It appears that a uniform weak hindrance of ~ 5 -10 relative to the Weisskopf estimate is a common feature for all neutron $M2$ transitions across the nuclear chart. This small hindrance was usually discussed in the literature as being possibly due to exchange current, core polarization, impure initial and/or final states, or relatively small shape changes between the initial and final states, see Refs. [13,14,16,48–51]. However, this hindrance might be a norm as the Weisskopf single-particle estimate was originally given in terms of proton transition [52].

5. Summary

In the present work, the decay of the $13/2^+$ isomeric state in ^{183}Hg populated in the α decay of the parent $13/2^+$ isomer in ^{187}Pb was identified for the first time. The half-life of this isomer

in ^{183}Hg was deduced to be $290(30) \mu\text{s}$, and its decay proceeds via a presumably delayed $M2$ transition (with yet unknown energy, denoted as Δ in the text) to the known $9/2^-$ member of the strongly prolate deformed $7/2^-$ [514] band, followed by a known prompt 105-keV $9/2^- \rightarrow 7/2^-$ transition. A lower limit of $B(M2, \Delta) \geq 0.018 \text{ W.u.}$ was deduced, which suggests a possible large hindrance with respect to the actually normal $13/2^+ \rightarrow 9/2^-$ $M2$ transitions in $^{175,177,179}\text{Hg}$, due to a substantial shape change between the parent and daughter states in ^{183}Hg .

Based on the analogy with ^{183}Hg , tentative evidence for a comparably strong hindrance is also proposed for ^{181}Hg , thus both $13/2^+$ isomers in these nuclei could be classified as shape isomers.

The $B(M2)$ systematics of normal neutron transitions across the nuclear chart is presented, which demonstrates the presence of a weak but global hindrance of ~ 5 -10 ($B(M2) \sim 0.1$ -0.2 W.u.) relative to the Weisskopf single-particle unit. Any larger hindrance factors could be related to a strong shape change in the decay and/or impure initial and/or final states, as for nuclei in Band B of Fig. 5.

Declaration of competing interest

The authors declare that they have no known competing financial interests or personal relationships that could have appeared to influence the work reported in this paper.

Data availability

Data will be made available on request.

Acknowledgements

This work has been supported by the Strategic Priority Research Program of Chinese Academy of Sciences (Grant No. XDB34000000), the National Key R&D Program of China (Contract No. 2018YFA0404402), the National Natural Science Foundation of China (Grants No. 12135004, No. 11635003, No. 11961141004 and No. 11735017). UK personnel are grateful for financial support from the STFC and A.N. Andreyev was partially supported by the Chinese Academy of Sciences President's International Fellowship Initiative (Grants No. 2020VMA0017). This work was also supported by the U.S. Department of Energy, Office of Nuclear Physics, under Contract No. DE-AC02-06CH11357 and Grants No. DE-FG02-94ER41041 (UNC) and DE-FG02-97ER41033 (TUNL), by the Slovak Research and Development Agency (Contract No. APVV-18-0268) and Slovak Grant Agency VEGA (Project 1/0651/21). This research used resources of ANL's ATLAS facility, which is a DOE Office of Science User Facility. The authors acknowledge the Target Labor team of GSI for preparing the targets for the experiment.

Appendix A. Supplementary material

Supplementary material related to this article can be found online at <https://doi.org/10.1016/j.physletb.2022.137345>.

References

- [1] O. Hahn, Über eine neue radioaktive Substanz im Uran, Ber. Dtsch. Chem. Ges. (A and B Ser.) 54 (6) (1921) 1131–1142, <https://doi.org/10.1002/cber.19210540602>.
- [2] P. Walker, Z. Podolyák, 100 years of nuclear isomers - then and now, Phys. Scr. 95 (4) (2020), <https://doi.org/10.1088/1402-4896/ab635d>.
- [3] P. Walker, G. Dracoulis, Energy traps in atomic nuclei, Nature 399 (6731) (1999) 35–40, <https://doi.org/10.1038/19911>.
- [4] G.D. Dracoulis, P.M. Walker, F.G. Kondev, Review of metastable states in heavy nuclei, Rep. Prog. Phys. 79 (7) (2016), <https://doi.org/10.1088/0034-4885/79/7/076301>.

- [38] R.B. Firestone, V.S. Shirley, C.M. Baglin, S.Y. Frank Chu, J. Zipkin, *Table of Isotopes*, 8th ed., 1996, New York.
- [39] T. Kibédi, T.W. Burrows, M.B. Trzhaskovskaya, P.M. Davidson, C.W. Nestor, Evaluation of theoretical conversion coefficients using BrIcc, *Nucl. Instrum. Methods Phys. Res., Sect. A, Accel. Spectrom. Detect. Assoc. Equip.* 589 (2) (2008) 202–229, <https://doi.org/10.1016/j.nima.2008.02.051>, <https://www.sciencedirect.com/science/article/pii/S0168900208002520>.
- [40] H. Huang, et al., Supplement, 2022.
- [41] T. Lönnroth, P. Ahonen, R. Julin, S. Juutinen, A. Lampinen, A. Pakkanen, S. Törmänen, W. Trzaska, A. Virtanen, Properties of the $13/2^+$ isomeric decay in ^{201}Hg , *Z. Phys. A* 337 (1) (1990) 11–14, <https://doi.org/10.1007/BF01283932>, <https://ui.adsabs.harvard.edu/abs/1990ZPhyA.337...11L>.
- [42] A.R. Poletti, G.D. Dracoulis, C. Fahlander, A.P. Byrne, The yrast spectroscopy of ^{209}Rn , *Nucl. Phys. A* 440 (1) (1985) 118–142, [https://doi.org/10.1016/0375-9474\(85\)90045-4](https://doi.org/10.1016/0375-9474(85)90045-4), <https://www.sciencedirect.com/science/article/pii/0375947485900454>.
- [43] P. Zeyen, K. Euler, V. Grafen, C. Günther, M. Marten-Tölle, P. Schüler, R. Tolle, Investigation of $^{203,205}\text{Hg}$ with the $(d, p\gamma)$ reaction – identification of the $i_{13/2}$ neutron hole state in ^{205}Hg , *Z. Phys. A* 325 (1986) 451–456, <https://doi.org/10.1007/BF01290048>.
- [44] W. Hua, X.H. Zhou, Y.H. Zhang, Y. Zheng, M.L. Liu, F. Ma, S. Guo, L. Ma, S.T. Wang, N.T. Zhang, Y.D. Fang, X.G. Lei, Y.X. Guo, M. Oshima, Y. Toh, M. Koizumi, Y. Hatsukawa, B. Qi, S.Q. Zhang, J. Meng, M. Sugawara, Properties of the rotational bands in the transitional nucleus ^{189}Pt , *Phys. Rev. C* 80 (2009) 034303, <https://doi.org/10.1103/PhysRevC.80.034303>.
- [45] S.K. Saha, M. Piiparinen, J.C. Cunnane, P.J. Daly, C.L. Dors, T.L. Khoo, F.M. Bernthal, High-spin levels in ^{191}Pt and ^{193}Pt and the triaxial rotor model, *Phys. Rev. C* 15 (1) (1977) 94–103, <https://doi.org/10.1103/PhysRevC.15.94>.
- [46] T. Kutsarova, C. Schück, E. Gueorguieva, A. Minkova, I. Zartova, F. Hannachi, A. Korichi, A. Lopez-Martens, Coexisting oblate and strongly triaxial structures in ^{191}Pt , *Eur. Phys. J. A* 23 (1) (2005) 69–78, <https://doi.org/10.1140/epja/i2004-10065-1>.
- [47] M. Piiparinen, S.K. Saha, P.J. Daly, C.L. Dors, F.M. Bernthal, T.L. Khoo, $\nu i_{13/2}$ and $\nu h_{9/2}$ isomers in odd-A Pt nuclei, *Phys. Rev. C* 13 (1976) 2208–2211, <https://doi.org/10.1103/PhysRevC.13.2208>.
- [48] M. Ramdane, P. Baumann, P. Dessagne, A. Huck, G. Klotz, C. Miehé, G. Walter, Identification of the $9/2^+$ to $5/2^-$ transition in ^{69}Se , *Phys. Rev. C* 37 (1988) 645–651, <https://doi.org/10.1103/PhysRevC.37.645>.
- [49] J.H. McNeill, A.A. Chishti, P.J. Daly, W. Gelletly, M.A.C. Hotchkis, M. Piiparinen, B.J. Varley, P.J. Woods, J. Blomqvist, Isomeric decay studies using a recoil mass separator, *Z. Phys. A* 344 (1993) 369–379, <https://doi.org/10.1007/BF01283192>.
- [50] C. Scholey, K. Andgren, L. Bianco, B. Cederwall, I.G. Darby, S. Eeckhaudt, S. Ertürk, M.B. Hornillos, T. Grahn, P.T. Greenlees, B. Hadinia, E. Ideguchi, P. Jones, D.T. Joss, R. Julin, S. Juutinen, S. Ketelhut, M. Leino, A.P. Leppänen, P. Nieminen, M. Niikura, M. Nyman, D. O'Donnell, R.D. Page, J. Pakarinen, P. Rahkila, J. Sarén, M. Sandzelius, J. Simpson, J. Sorri, J. Thomson, J. Uusitalo, M. Venhart, Isomeric and ground-state properties of $^{171}_{78}\text{Pt}$, $^{167}_{76}\text{Os}$, and $^{163}_{74}\text{W}$, *Phys. Rev. C* 81 (1) (2010) 014306, <https://doi.org/10.1103/PhysRevC.81.014306>.
- [51] R. Barden, A. Plochocki, D. Schardt, B. Rubio, M. Ogawa, P. Kleinheinz, R. Kirchner, O. Klepper, J. Blomqvist, Beta-decay of $27/2^-$ isomers in $n=83$ nuclei, *Z. Phys. A* 329 (1988), <https://doi.org/10.1007/BF01294811>.
- [52] V.F. Weisskopf, Radiative transition probabilities in nuclei, *Phys. Rev.* 83 (1951) 1073, <https://doi.org/10.1103/PhysRev.83.1073>.